The FTire Tire Model Family

Michael Gipser
Esslingen University of Applied Sciences, Automotive Engineering Department
Esslingen, Germany

1 Modelization

Being a typical representative of detailed mechanical tire models 'below' true FEM models, the author's model family FTire (Flexible Ring Tire Model) will be discussed in greater detail here. FTire development started in 1998, using certain ideas and numerical concepts of the author's 'coarse-mesh' FE model DNS-Tire ([1], [2], [4]) and the spatial non-linear 'rigid-ring' model BRIT ([3], [5], [6]). This first version of FTire has been essentially improved since then. It is one of the advanced tire models of MSC.ADAMS™, and is as well implemented into several 'in-house' simulation programs at different companies, and as a sub-system block in MATLAB/SIMULINK™. Recently, FTire has been completed by a new rigid-ring model (called RTire), and a redesign of DNS-Tire (called FETire). RTire, FTire, and FETire together set up the FTire Model Family. FTire and FETire are discussed below.

1.1 FTire: Flexible Ring Tire Model

FTire is the most important member of the FTire model family. Like most other mechanical tire models, the kernel of FTire consists of two separate parts. The first part is describing the tire's structural stiffness, damping, and inertia properties (the structure model, for short). The second one is the tread/road contact model, comprising road evaluation, and computation of contact pressure distribution and distributed friction forces (the tread model, for short).

Underlying idea of the structure model is to introduce only as few degrees of freedom as necessary, to represent all tire properties that are relevant for the application. Main objectives during development had been:

- fully non-linear 3D model, working in time domain;
- valid up to 150 Hz both in-plane and out-of-plane;
- longitudinal wave lengths ≤ 5 cm, including sharp-edged obstacles;
- lateral wave-lengths ≤ 15 cm;
- parameterization as easy and flexible as possible;
- usage of 'easy-to-measure' static, steady-state, and modal properties in parameterization;
- computing time ≤ 5 .. 20 times real time;
- valid for ride and handling, both in steady-state and dynamic conditions;
- simple and flexible interfacing to vehicle and road models.

Potential applications of FTire comprise of

- tire models for passenger cars, motor-cycles, race cars, trucks, trailers, ATVs, aircrafts, earth-moving machines, etc.;
- all vibrations up to about 150 Hz, induced by tire/road contact;
- vibration excitation through tire imperfections;
- generation of load histories for durability simulations;
- traction and handling on extremely uneven roads;
- rolling resistance studies on even and uneven road;
- tire misuse;
- steering torque amount when parking;
- assessment of highly dynamic suspension control systems;
- moving ground, all kinds of test-bench simulations;
- tire temperature and its influence on road friction;
- tread wear; and
- sudden pressure loss.

Most model extensions, like thermal and wear model, tire misuse, and tire imperfections have been stimulated by users in vehicle and tire industry. Of course, there are still many effects which are of relevance in suspension design and optimization, but cannot be analyzed using FTire, like noise generation, traction on soft soil or snow, hydroplaning, and more.

1.1.1 Structure Model

The FTire structure model consists of 80 to 200 lumped-mass nodes, replacing the tire's steel cord. These nodes are connected to the rim and to each other by several non-linear, inflation pressure dependent stiffness, damping, and friction elements. Moreover, the nodes are subject to inflation pressure forces in radial

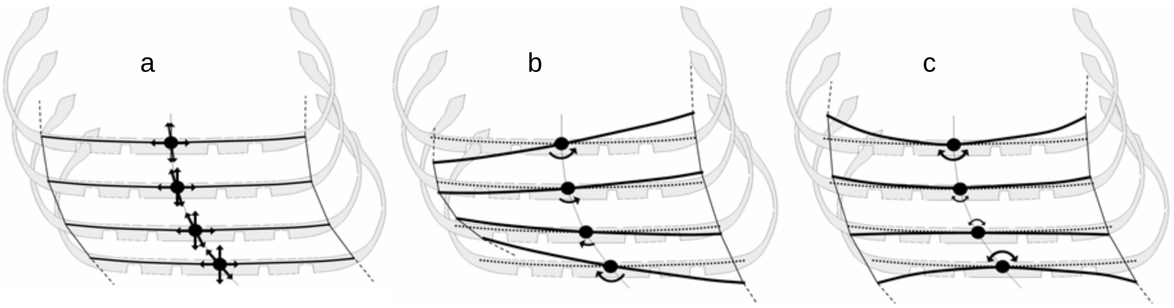

Fig. 1: Belt Segments' Degrees of Freedom: (a) Translation, (b) Torsion (c), Lateral Bending

direction, and to the forces of the tread model. The part of the tire structure which is associated to one such belt node is called belt segment. Each belt segment has 5 degrees of freedom (figure 1):

- longitudinal, lateral, and vertical displacement,
- rotation angle about the circumferential axis ('belt torsion'), and
- bending in lateral direction, perpendicular to the circumferential axis.

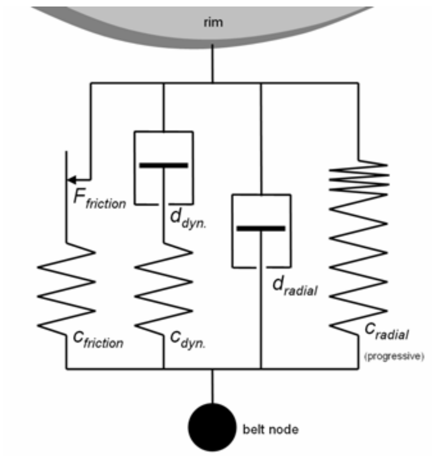

Fig. 2: Radial Force Elements between each Belt Node and Rim

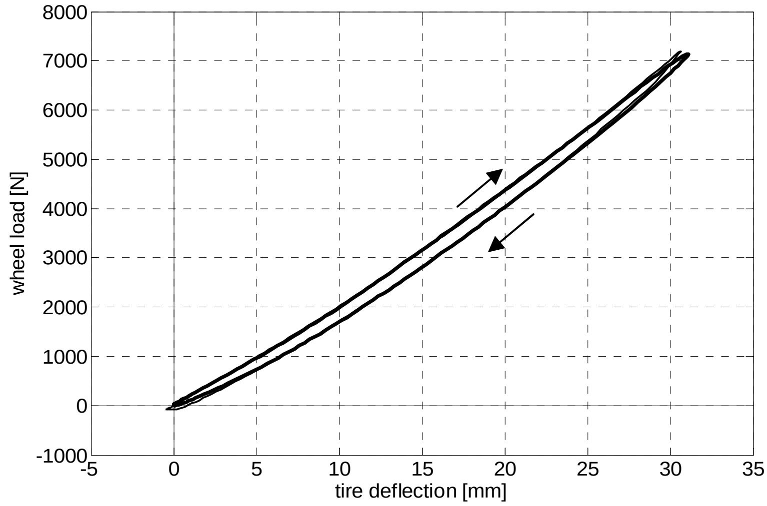

Fig. 3: Measurement (bold line) and FTire simulation (thin line) of Radial Tire Characteristic with Hysteresis

The elastic coupling between belt nodes and rim is described by nonlinear force elements in radial, circumferential, and transversal direction, comprising springs, dampers, Maxwell elements and spring-friction series connections (‘elasto-plastic’ elements). Figure 2 shows the radial force element of one single belt node; circumferential and transversal elements are placed analogously. Maxwell elements are used to describe the ‘tire stiffening’ at higher rolling speeds, whereas the dry friction element replaces rubber hysteresis. The effect of this hysteresis on overall tire radial stiffness can clearly be seen in measurements, as well as corresponding FTire simulations (figure 3).

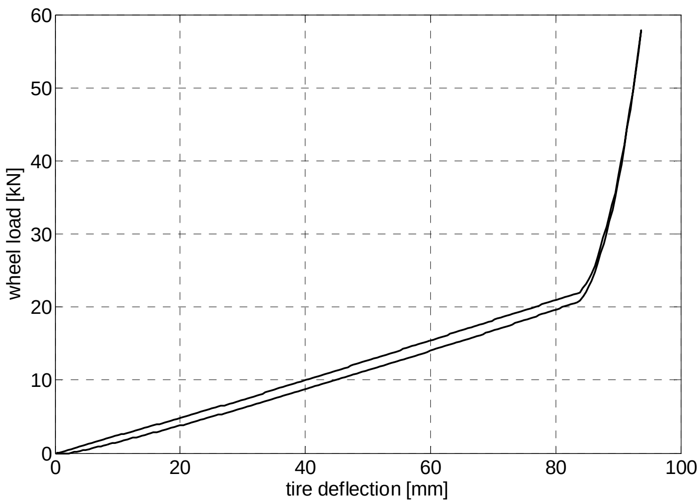

Fig. 4: Progressive Radial Stiffness due to Rim Flange Contact

The radial stiffness elements are completed with unilateral stiff springs, located along the radial direction at the rim flanges. When tire deflection exceeds a certain value, these springs will come into contact with the inner side of the belt, thus generating an extremely progressive radial stiffness characteristic (figure 4). Depending on camber angle, this rim-to-belt contact can happen on one rim flange only, or on both at the same time. Rim-to-belt contact enables to simulate certain tire misuse situations.

In addition to the translational force elements, a torsional spring $c_{torsion}$ (cf. figure 5) is located between each belt segment and the rim. These torsion springs serve as ‘elastic foundation’ of the belt segments torsion degree of freedom. Moreover, a bending stiffness acts against lateral belt bending. Together with the radial stiffness, they describe left and right side-wall stiffness.

The following additional force elements are connecting neighbouring belt nodes:

- a very stiff translational spring c_{long}, (figure 5), providing the belt extension stiffness,
- another torsional spring, connecting the torsion degree of freedom of two adjacent nodes (this spring is not depicted in figure 5),
- a bending stiffness $c_{bend,in-plane}$ (figure 5), connecting three nodes in line, acting against belt bending perpendicular to the lateral axis (‘in-plane bending stiffness’), and
- another bending stiffness $c_{bend,out-of-plane}$ (figure 5), acting against belt bending perpendicular to the radial axis (‘out-of-plane bending stiffness’).

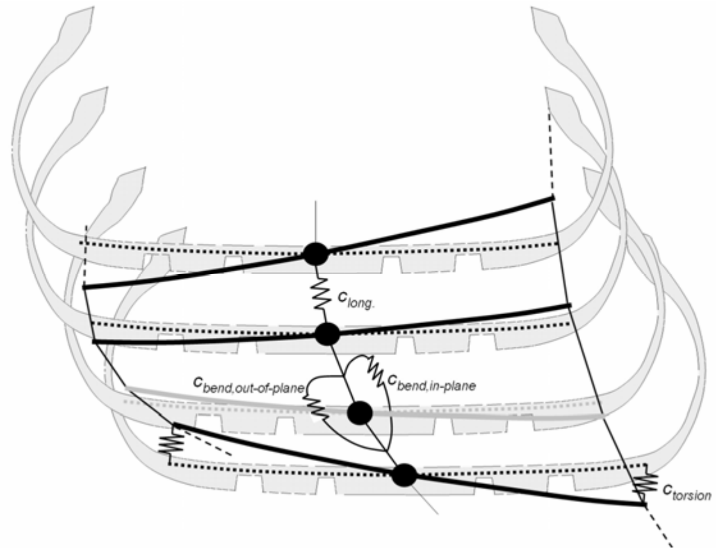

Fig. 5: Belt Flexibility Stiffnesses

All stiffness values depend on the actual inflation pressure. The pressure is treated as an ‘operating condition’ and might be arbitrarily changed during a running simulation. This will not disturb the integration process in any way. Moreover, actual inflation pressure depends on tire temperature, which is the output of the thermal model (cf. chapter 1.1.3). Inflation pressure does not only affect the stiffness values, but generates extra forces, which act on the belt nodes in radial direction. These forces generate a membrane tension, by expansion of the longitudinal springs. This leads to a further ‘stiffening’ of the steel belt, similar to that one caused by the in-plane bending stiffness.

Figure 6 shows the first eigenvalues of the linearized structure model, for three different radial deflection values. The linearization technique applied here can be used to compute transfer functions under different operating conditions as well.

The structure model may be completed by specifying several types of imperfections, to better match a real tire. These imperfections comprise: static and dynamic imbalance, radial and tangential non-uniformity, ply-steer, conicity, and geometrical run-out.

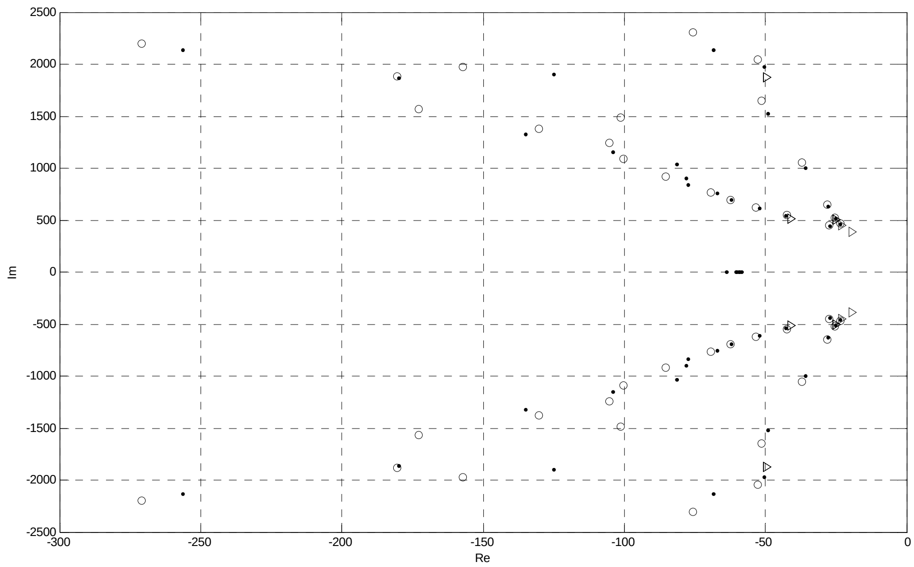

Fig. 6: FTire Eigenvalue Location of Linearized Structure Model; ▷ unloaded tire; • 20 mm deflection; O 40 mm deflection; real and imaginary axes are scaled differently

1.1.2 Tread Model

Between two neighbored belt segments, there are placed a certain number of mass-less contact and friction elements, to establish road contact (figure 7). Their number, between 5 and 50, can be selected by the user, depending on the desired road irregularity resolution. These contact elements constitute the tread model.

The contact elements are either placed along parallel lines, or are distributed randomly, extending over the tread width. The exact positions at which the contact points are attached to the belt segments are smoothly interpolated, using the co-ordinates of the four nearest-by belt nodes, as well as the actual belt's cross-section geometry. Vice versa, the forces that are generated by the contact elements will contribute to the external forces of all four belt nodes. The actual belt's cross section geometry is defined by all degrees of freedom of the two nearest-by belt nodes.

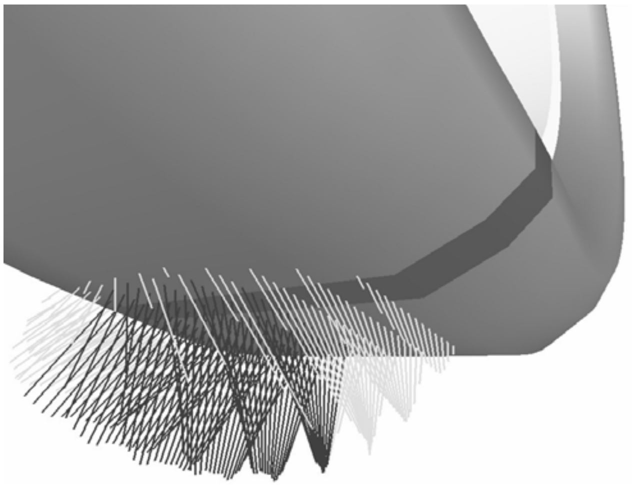

Fig. 7: Distributed Contact Forces during Parking Manoeuvre

If the tread pattern is given in terms of a black-and-white bitmap file, the contact elements' lengths (that is, the local tread rubber height) may be set according to this pattern. In figure 8, the computed contact pressure of such a model is shown. Here, 120 segments and 50 contact elements had been used; the contact elements are placed along 25 parallel lines. This resulted in a tread resolution of approximately 0.5 x 12 mm for the large truck tire. Clearly, it would require an unacceptably large amount of contact elements to exactly resolve more complicated patterns, like for example those of passenger-car tires.

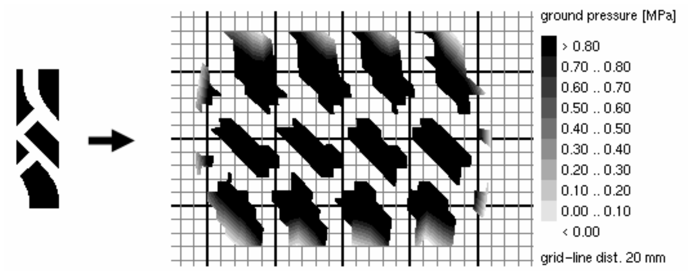

Fig. 8: Tread Pattern Bitmap and Resulting FTire Contact Pressure Distribution

During any integration step, for each contact element a rapid test is performed to check whether the element might have road contact. This test uses the position of the nearest-by belt element. If the test is passed, the exact distance of the contact element to the road surface is computed. Only if the contact element penetrates the road, the contact computation will be continued by determining the road surface tangential plane, the deflection, the resulting normal force, and more.

The road tangential plane is computed individually for each contact element, by evaluating the road height in three different locations near the contact element. This is necessary to resolve even sharp-edged obstacles, like cleats and pot-holes. Road surface may depend on time, like it does for four-post test-rigs and rotating drums. In that case, both normal and tangential surface velocity is taken into account as well.

The normal force is a function of deflection and deflection velocity, describing tread rubber compression stiffness and damping. These values, in turn, are determined on basis of the tread rubber's Young's modulus, the tread pattern's net-to-gross ratio, the local tread depth, and more. Clearly, pressure distribution and thus normal force strongly depends on the tire's cross section geometry; most of all on the belt curvature in unloaded condition, as well as on tread depth as function of the lateral co-ordinate. This is why this geometric data can be prescribed in a very detailed way, by using look-up tables with smooth spline interpolation.

After having computed the normal force, in the next step the vector-valued friction force in the tangential plane is determined. Its absolute value is given by

$$\left|F_{friction}\right| = \mu(v_{slide}, p_{ground}, T_{tread}) \cdot F_{normal} \,,$$

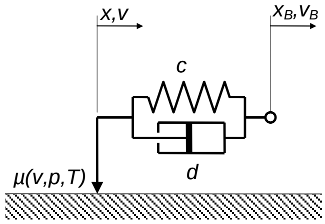

Fig. 9: Contact Element Tangential Displacement Model

whereas the direction is the negative sliding velocity direction. Sliding velocity is determined by using the vector-valued force equilibrium condition of friction force, elastic shear forces, and shear damping force of the contact element (figure 9) in the road tangential plane.

This force equilibrium condition results in a differential equation for the element's tangential displacement. Depending on the nature of the friction coefficient as function of sliding velocity, this differential equation might have a discontinuous right-hand side, or, even worse, might be unstable. The only way to numerically solve such an equation is using implicit integration. It turns out that this integration requires an additional discrete state variable, which memorizes whether the element was sticking to ground, or sliding, in the previous time step.

1.1.3 Thermal Model and Wear Model

The tread model is completed by a thermal model and a model for tread wear estimation. The thermal model consists of

- the thermo-dynamical computation of the actual inflation pressure as function of filling gas mass, 'cold tire inflation pressure', tire temperature, and actual interior volume, and
- a heat generation and transfer model, introducing state variables for the temperature of the tire structure (including filling gas), and the individual temperature of each tread contact element. Heat generation and transfer are driven by the power loss distribution due to structural damping and dry friction on the road surface. As already mentioned, tread temperature influences road friction coefficient.

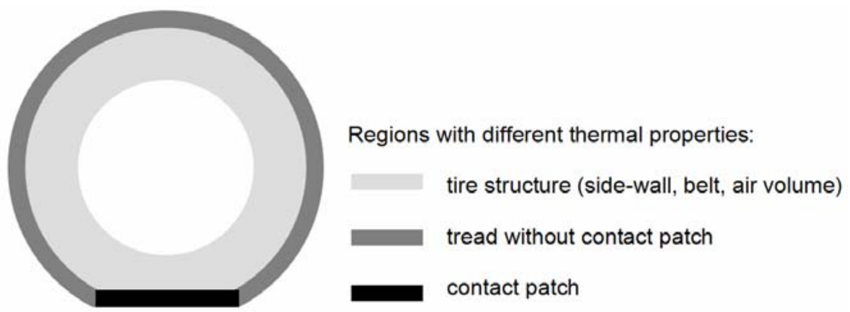

Fig. 10: Regions of the Thermal Model

In the heat generation and transfer sub-model, the tire is assumed as being separated into three regions, having different thermal properties each (figure 10): the tire structure (including bead, side-walls, belt, and air volume), the tread without contact patch, and the contact patch. The following assumptions are made for the three different regions.

The tire structure is described by one global temperature only. The product of rate of change of this temperature and the tire structure's overall heat capacity is balancing the sum of

- the power loss in all energy dissipating force elements in the belt and side-wall, excluding friction and damping of the tread elements;
- the heat which flows from the tire structure into the two tread regions. This heat transfer is determined by the respective temperature differences, multiplied by an appropriate heat transfer coefficient. This heat transfer coefficient is assumed to be independent on rolling speed;
- the heat which is transferred from the side-walls into the air flowing around the tire. This transfer is determined by the temperature difference between tire structure and ambient air, multiplied by an appropriate heat transfer coefficient. This heat transfer coefficient is assumed to be strongly and nonlinearly dependent on rolling speed.

The tread without contact patch is described by a distributed temperature, assigning one value individually to each tread element. The product of rate of change of this temperature and the tread element's heat capacity is balancing the sum of

- the power loss in the tread element due to material damping;
- the share of the heat which flows from the tire structure into the particular tread element, as already described above;
- the heat being transferred from the tread element to the air flowing around the tire. This heat transfer is determined by the temperature difference between tread element and ambient air, multiplied by an appropriate heat transfer coefficient. Again, this heat transfer coefficient is assumed to be strongly and nonlinearly dependent on rolling speed, but has the same value for all elements not in contact to the road.

The contact patch is described in a similar way like the remainder of the tread, with the following exceptions: additional power loss due to road friction is taken into account, and heat is transferred to the road instead of the surrounding air. Heat transfer coefficient between tread and road is assumed to be independent on rolling speed.

As an example, figure 11 shows the resulting temperature distribution in contact patch, after 2 s cornering at 4 kN wheel load, 4 deg camber angle, and 8 deg side-slip angle.

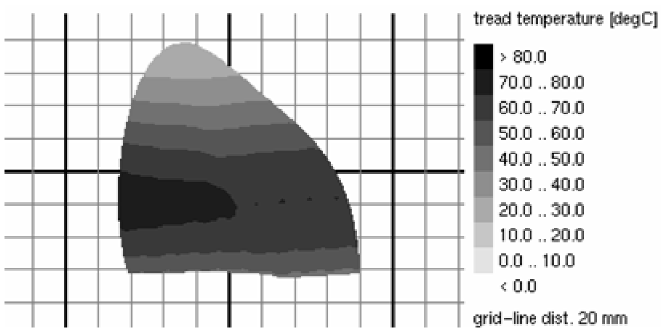

Fig. 11: Temperature Distribution in Contact Patch during Cornering at 6 deg Camber Angle

The tread wear model uses the friction power (which is the product of friction force and sliding velocity), and a functional relationship between friction power and wear rate. These variables are used to update, individually for each contact element, the actual local tread depth:

$$\dot{d}_{tread} = -f_{wear}\left(\left|F_{friction}\right| \cdot \left|v_{slide}\right|\right)$$

Accompanied by this reduction in tread depth, all tread properties that depend on tread depth will be modified respectively: compression stiffness and damping, shear stiffness and damping, heat capacity, and tread mass distribution. Thus, even imbalance and run-out caused by a locked braking will be seen as result of a respective simulation experiment. Clearly, both the thermal and the wear model can be deactivated. Constant temperature and constant tread depth will be used in that case.

1.1.4 Model Data and Parameterization

As already discussed in chapter 1, ease of parameterization is one of the most important objectives of any tire model, and this of course holds for FTire as well. Here, a clear distinction is made between data used in the model equations ('pre-processed data'), and data to be supplied by the user ('basic data'). The underlying idea is to define basic data which is as easy as possible to obtain, and which at the same time yield complete information to determine the pre-processed data in a unique way. The more direct as well as sensitive single pre-processed data items depend on only few basic data, the more robustly, reliably and rapidly pre-processing will perform.

This pre-processing requires the solution of several nonlinear systems of equations, and will take some seconds of computing time. After successful completion, the resulting internal data is appended to the basic data in the data file. When using this data file the next time, it will be checked whether basic data has been changed in any way. If not, pre-processing phase is skipped, using the appended data instead.

Whether parameters are 'easy to obtain' might be seen very different by different users. What is 'easy' at one test facility might be difficult or impossible to get at another one. This is why there are different alternatives and combinations for some of the basic data, especially for that of the structure model. Moreover, not all data items are equally relevant for all applications. For example, in many cases belt out-of-plane bending stiffness does not affect the tire response when rolling over a transversal cleat, and the friction coefficients nearly do not influence the radial tire characteristic.

Besides elementary data like tire and rim size, load index, speed symbol, mass, and rolling circumference, the structure model requires one out of several different combinations of static and modal data of the total tire. During pre-processing, the corresponding internal stiffness, damping, and inertia data are determined such that the resulting FTire model shows exactly this prescribed global behavior.

The following data enumeration only reflects one possible such combination. A comprehensive and up-to-date list of all data items can be found at www.ftire.com. Tools to assist in parameterization will be discussed in chapter 7. A typical FTire parameterization uses

- tire size, load index, and speed symbol
- rolling circumference
- tire mass
- rim diameter and rim width
- tread width and tread depth as function of lateral tread co-ordinate
- distance of tread grooves to steel belt (‘cap base height’)
- tread pattern net-to-gross ratio (alternatively, tread pattern bitmap file)
- mean lateral belt curvature radius of the unloaded tire’s cross-section (alternatively, detailed spline data of cross section geometry)
- Young’s modulus of tread rubber
- tread rubber adhesion friction coefficient for one up to three contact pressure value(s)
- tread rubber sliding friction coefficient for two sliding velocities and one up to three contact pressure value(s)
- natural frequencies and modal damping of vibration modes 1, 2, 4, and 6 (cf. figTure 12), for an unloaded, inflated tire with fixed rim, for one or two inflation pressure value(s)

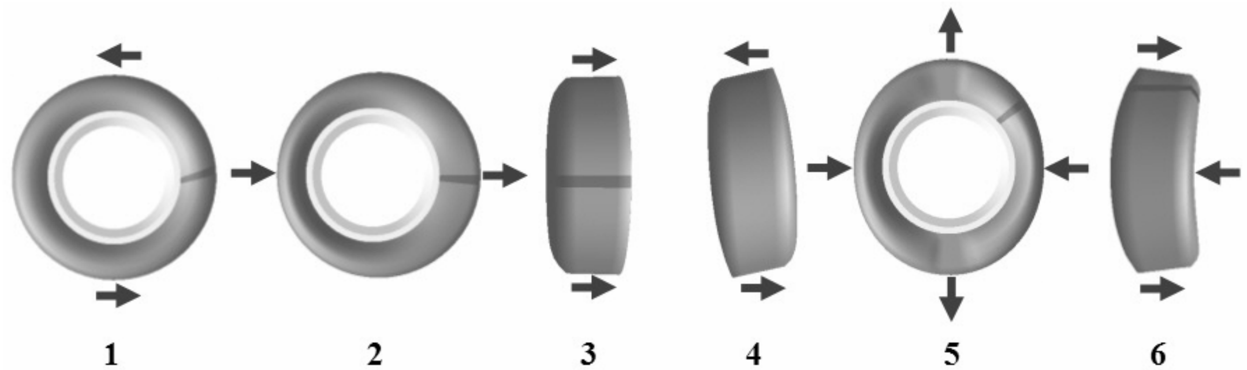

Fig. 12: First Unloaded Vibration Modes for Use in FTire Parameterization and Validation

- vertical force
  - o of standing tire on a flat surface, for two deflection values and one or two inflation pressure value(s)
  - o of standing tire, both on a transversally and a longitudinally oriented cleat, for one or two inflation pressure value(s)
  - o of standing tire at large camber angle, both on flat surface and a transversally oriented cleat, for one or two inflation pressure value(s)
  - o of rolling tire on flat surface, for two different rolling speeds.

1.1.5 Numerical Aspects and Implementation

As discussed in chapter 4, tire models need to be very versatile with respect to the calling MBS software and the computing environment. For that reason, FTire is implemented in standard Fortran 90 (a Fortran 77 version being also available), together with an interface for C and C++ solvers. Both the Fortran and C interface to the calling MBS solver is organized in terms of an API (Application Programming Interface), and compiled for all important Windows™- and Unix-type operating systems. Seemingly arbitrarily many instances of the model can be simulated at the same time, without interfering with each.

The numerical integration basically is performed in two steps for each time increment. This time increment might be of fixed or variable length. It will be automatically subdivided into smaller steps if rim rotation increment exceeds a certain angle threshold (1 degree, say). Thus, FTire can be easily linked to MBS software which uses step-size controlling integrators, and yields sufficient accuracy independent on rolling speed. As with all highly dynamic sub-systems, the MBS solver's integrator should be configured to limit the communication interval between MBS model and tire model to a reasonable value. In the case of FTire, a value less or equal to 1 ms is recommended. Otherwise, the MBS model cannot accurately follow any high-frequent tire excitation. Just one number might illustrate this: the tire's total contact time to a cleat, run over at a speed of 200 kph, is less than 4 ms. Even though FTire accumulates the forces of the internally used smaller steps, the feed-back due to the change in rim velocity is decisive as well.

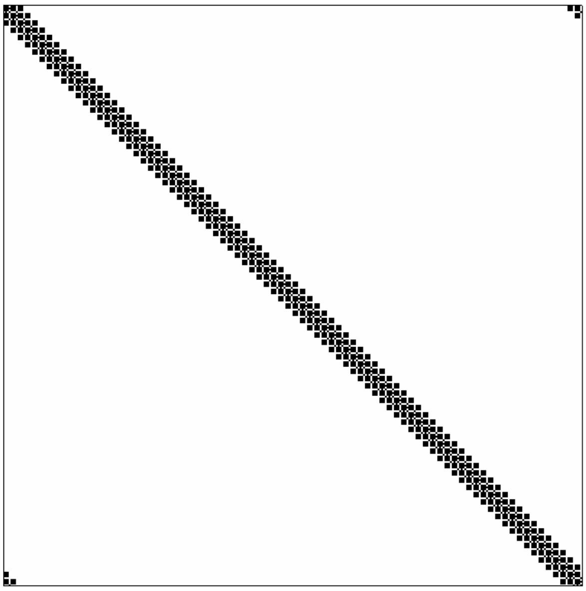

Fig. 13: Sparsity Pattern of Stiffness Matrix

In the first step of each local time increment, the contact processor is called. It will perform all necessary updates of the tread-model related state variables, and compute the generalized forces that act between tread rubber and belt segments. The contact processor also calls the road evaluation routine, to determine location- and time-dependent road height and friction value modification. A simple program interface to these evaluation routines was chosen, to enable the connection of FTire to a wide variety of user-written and application-specific road implementations.

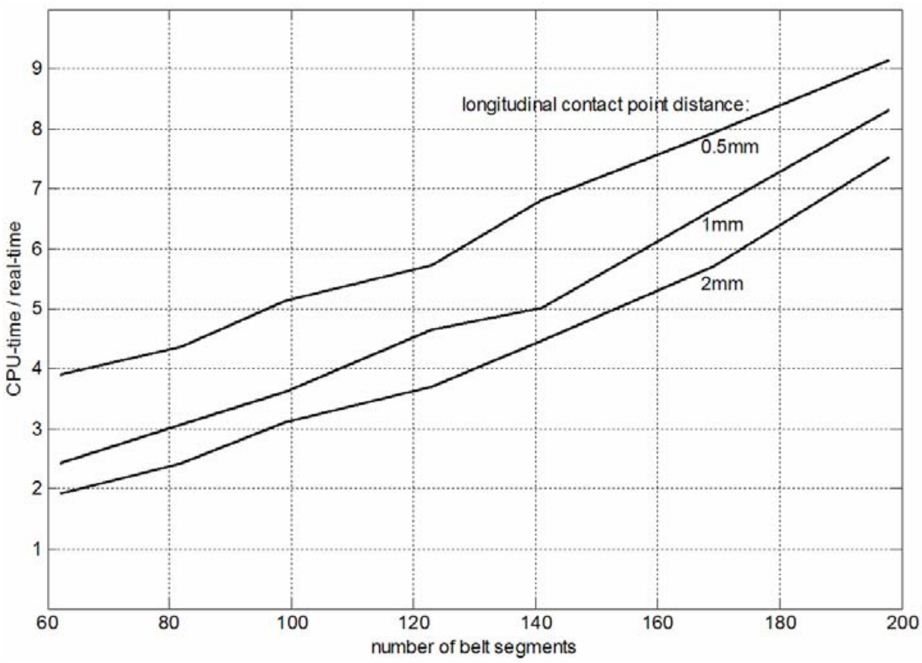

Fig. 14: CPU-Time of FTire, Depending on Belt Segments and Contact Patch Resolution

In the second step, the tire structure model is updated. The size of this system is determined by the number of the belt segments' degrees of freedom. Integration is done by a slightly modified implicit trapezoidal scheme, which in turn is a special case of the widely used Newmark integration. This integrator requires certain system Jacobians: the matrices of partial derivatives of acceleration variables with respect to position and velocity states. These matrices, being closely related to the linearized structural stiffness and damping matrices, are extremely sparse. Moreover, even though they depend on the actual values of the tire structure states, they can be computed analytically in only short extra computing time. Figure 13 shows the non-zeros pattern ('sparsity pattern') of these matrices, which are so-called cyclic band matrices, in the case of 80 belt segments. Only 3.9 % of all matrix elements are non-zero. Even after Cholesky-factorization, this value is only about 7.8 %. This is important because the number of arithmetic operations to solve the system is closely related to the number and location of non-zero elements of the Cholesky factor.

Figure 14 shows the resulting measured CPU-time of FTire, in dependency on both the longitudinal contact element distance (which determines the spatial contact patch resolution), and the number of belt segments. Computations had been performed on a 3GHz Pentium M™ processor under Windows XP™ operating system, using Compaq Visual Fortran™ 6.6B compiler. Time step had been 0.5 ms. Thus, the maximum visible frequency was about 0.5 kHz. The diagram shows the real-time factor RTF, which is the quotient of CPU time to real time. Apparently, computing time depends nearly linearly both on the number of belt segments and on the number of contact elements. For a reasonable numerical tire discretization (80 belt segments and 1 mm contact patch resolution), RTF is close to 3.

More about FTire, including a free evaluation version and several validation results, can be found at [11].

1.2 FETire: Coarse-Mesh FE Tire Model

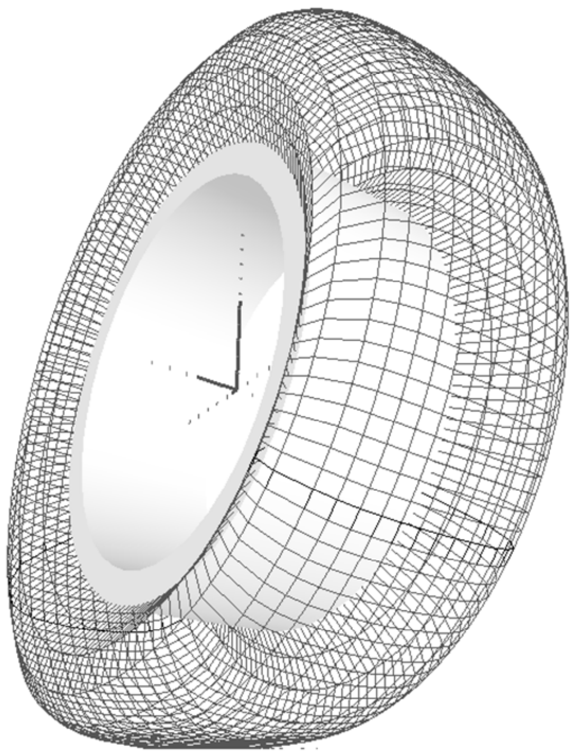

Fig. 15: FETire: Mesh of Structure Model

As mentioned above, FTire is completed with a 'coarse-mesh' finite element model (FETire), and a 'rigid-ring' model (RTire). All the members of this FTire model family, being of very different complexity, use exactly the same program interfaces, and are designed to be data-compatible as far-reaching as possible. At present, FTire is understood as the most important member of the model family, because it seems to be the best compromise between application range, accuracy, and computing time for most vehicle dynamics investigations.

FETire, on the other hand, requiring about 50 to 100 times more CPU time than FTire, today is mainly used for

- assistance in the parameterization of FTire,

- theoretical investigations on tire response to ‘non-standard’ excitations, and
- studies about influence of tire design characteristics to handling and ride comfort properties.

However, with ever growing computing power, and complexity of suspension models, FETire might be used more widely in the future, even with full vehicle models. Real-time factor is about 300 at present, so 10 s simulation of a full vehicle completely equipped with FETire, would take about 4 h CPU time. This might be a tolerable effort for occasional or special investigations.

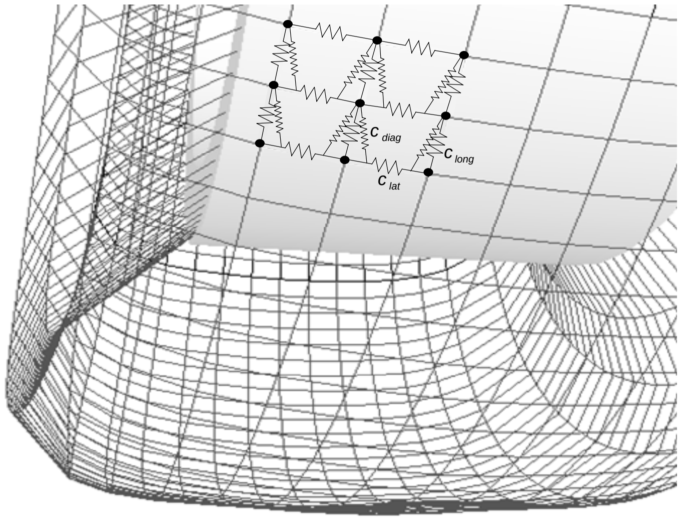

Fig. 16: Springs Replacing Anisotropic Membrane Stiffness

Similarly as FTire, FETire comprises a structure model and a tread model. The structure model (figure 15) uses some 1000 to 5000 lumped-mass nodes, having three translational degrees of freedom each, and being connected by a non-linear network of springs and dampers (figure 16). This coarse finite element mesh is automatically generated, using the cross section geometry of the unloaded and uninflated tire only. The distributed membrane stiffness and damping of the layered tire shell structure, consisting of carcass layers, belt layers, bandage layer, bead filler, etc., is computed during pre-processing. It is replaced by the above mentioned anisotropic, geometrically fully nonlinear spring and damper network (dampers not displayed in figure 16). Stiffness and orientation of the springs is computed such that the resulting linearized stiffness matrix exactly coincides with the membrane stiffness matrix of the layered structure, separately in each cross section region. By this procedure, for example, very stiff springs are created in the belt region, following the two belt cord direction angles (c_{diag} in figure 16).

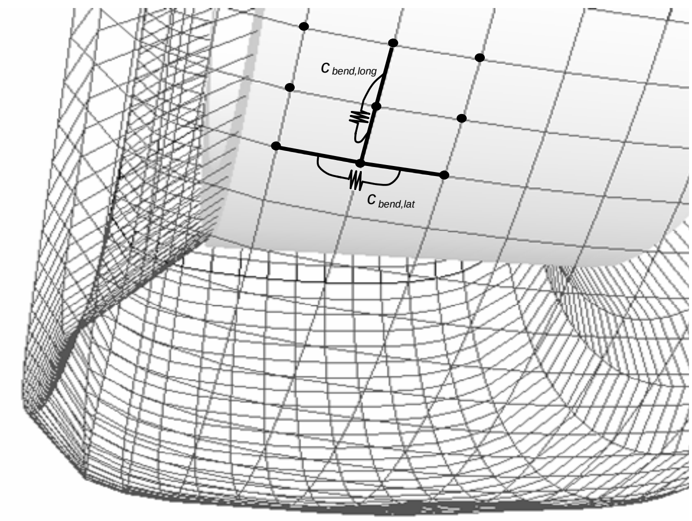

Fig. 17: Longitudinal and Lateral Bending Stiffness in Shell Structure

This membrane stiffness model is completed by the plate stiffness model, which uses discrete bending stiffness elements. These elements connect any three longitudinally and laterally neighbored nodes in the belt and side-wall region (figure 17).

Finally, radial forces due to inflation pressure contribute to the nodal forces. They act along the shell normal direction, being in turn a nonlinear function of all neighbored node positions. Inflation pressure is computed as thermodynamic function of inner volume and air temperature. Inner volume, in turn, is a simultaneous function of all shell node positions.

Similarly as with FTire, a highly specialized Newmark-type implicit integration is applied to the nodal degrees of freedom. This integrator takes full advantage of the sparsity pattern of the system Jacobian, and exploits the fact that the tire structure undergoes largest strains in the vicinity of the contact patch only.

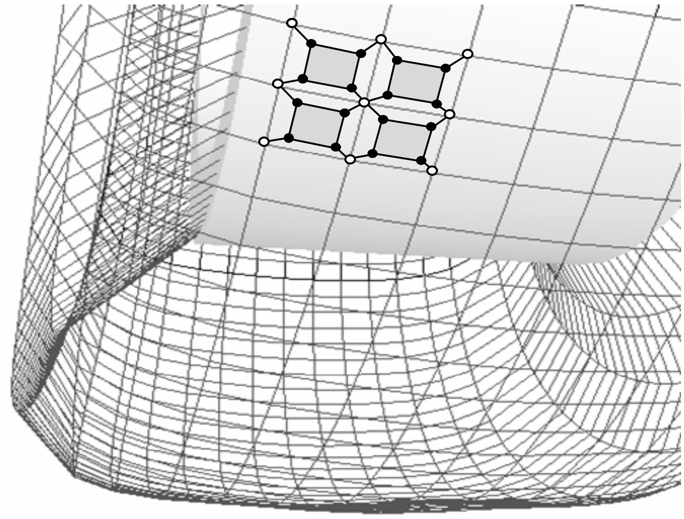

Fig. 18: Tread Nodes (●) with Associated Shell Nodes (○)

In contrast to FTire, the tread model consists of finite elements that are equipped with mass (figure 18). To each quadruple of neighbored shell nodes in the belt region (○), a certain number (4, say) of tread nodes (●) is associated. These tread nodes are coupled by a nonlinear radial and tangential stiffness each to their four associated shell nodes. The treatment of road contact and friction is essentially the same as in FTire.

There are two special versions of FETire available. FETire/modal performs linearization and modal analysis of the unloaded tire (figure 19). FETire/static is used for rapid non-linear static load-case calculation of the loaded but standing tire (figure 20). The latter uses mesh refinement near the contact patch. For rolling tires, this refinement would lead to an unacceptable computational overhead when shell nodes enter or leave the refinement region.

Both special versions are optimized for CPU time, and can be used to assist in FTire parameterization (cf. section 7).

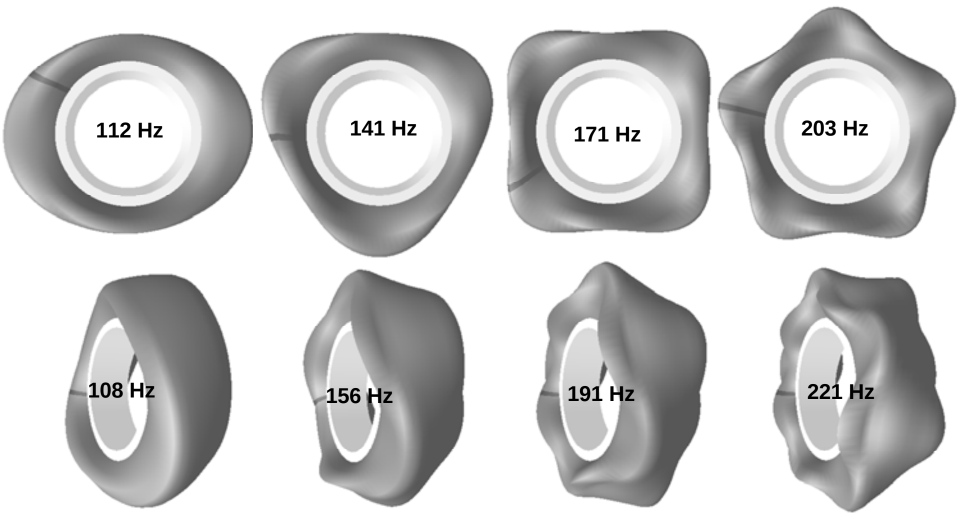

Fig. 19: FETire/modal: First Eight In-Plane and Out-of-Plane Bending Modes of an Unloaded Passenger Car Tire. 5130 degrees of freedom, 6 s CPU time for all modes

To compute stiffness data of the shell structure, FETire uses a parameterized description of the plies and all other important tire compounds. This description is implemented in terms of template files, called tire-design data files. Each tire-design data file qualitatively describes a certain class of tires, like passenger car tires, motor-cycle tires, and so on. In such a file, the tire's cross section is separated into several regions, like bead core, apex, side-wall center, shoulder, belt zenith, etc. Associated to each region, there is a layer list, enumerating each layer together with is thickness, matrix rubber stiffness, cord stiffness (if any), and cord thread angle. Figure 21 shows an example of such a layer list.

A layer list does not contain numerical values, but rather few variables only. The actual values of these variables, like belt cord density, belt cord direction angle, layer height, etc., together with a spline-based description of cross section geometry and tread depth finally are added to the tire-design data file to describe a specific tire. To a certain degree, this approach allows a very simple extrapolation, starting from the data of one tire size to estimate the data of another, similar one.

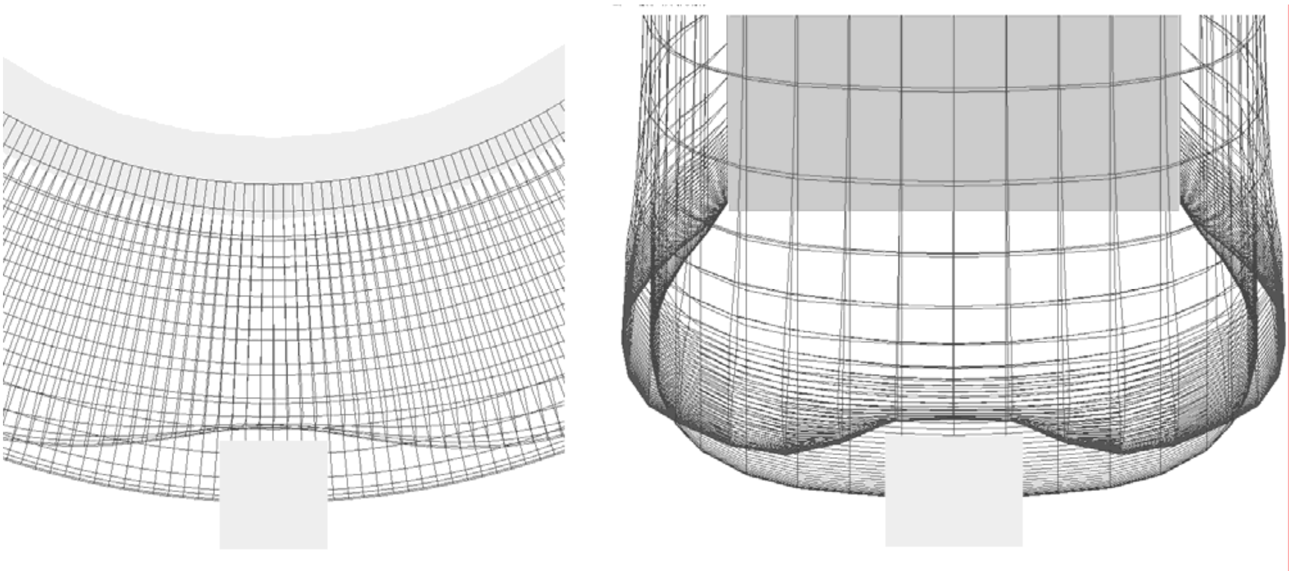

Fig. 20: FETire/static: Load-Cases ‘Transversal Cleat’ and ‘Longitudinal Cleat’.
Deflection 35 mm, structural distortion compared to that of unloaded tire. 6750 degrees of freedom, 92 s CPU time per load-case

```
$layer_list_8 ! belt zenith ******************************************
*---------------------------------------------------------------------
* cr.sect. cord dens. height   alpha       E cord E matrix  type
* mm^2     thr/mm     mm       deg         N/mm^2 N/mm^2
*---------------------------------------------------------------------
s_belt = 0.5
  0.0      0.0        h_il      0.0        0.0    E_il   ! inner liner
  A_carc   d_carc     h_carc    ang_car1   E_carc E_cp   ! 1. body ply
  A_carc   d_carc     h_carc    ang_car2   E_carc E_cp   ! 2. body ply
  A_belt   d_belt     h_belt    ang_belt   E_belt E_bp   ! 1. belt ply
  A_belt   d_belt     h_belt   -ang_belt   E_belt E_bp   ! 2. belt ply
  A_carc   d_band     h_band    0.0        E_carc E_b    ! 1. bandage
  A_carc   d_band     h_band    0.0        E_carc E_b    ! 2. bandage
  0.0      0.0        h_base    0.0        0.0    E_tr   ! tread base
```

Fig. 21: Single Layer List of a Passenger Car Tire-Design Data File

Of course, the accuracy of FETire does not reach that of detailed FE models. FETire is proven compromise between accuracy and computational efficiency. It is of value as long as detailed FE models can not yet be used, for many different reasons, in time-domain non-linear vehicle dynamics simulations.

2 Parameterization Tools

Parameterization of any tire model, as mentioned above, always is a delicate task. Basically, there are five different procedures used in practice:

(1) direct determination of parameters by using appropriate measurements, or

(2) usage of a detailed FE model, together with a 'condensation process', to directly compute the parameters, or
(3) usage of measurements of the global tire behavior to estimate the model parameters by means of least squares approximation ('parameter identification'), or
(4) performance of simulations with a detailed FE model, to generate 'virtual measurements', subsequently used for parameter identification as in (3), or
(5) usage of a well-validated data file, and application of certain 'extrapolation formulae' to estimate the tire data of another size, 'not too far away' from the validated size.

Clearly, due to the different nature of model parameters, none of these five procedures will be used unadulterated. Some data will always be measurable directly, like for example simple geometric properties that are only depending on tire size, or on tread rubber friction coefficients. Some other data can never be determined directly, for example something artificial like 'the stiffness matrix coupling two adjacent belt segments'. For the FTire model family, as an example, tools that assist with procedures of type (3), (4), and (5) are available, cf. figure 22.

The first one, called FTire/calc, performs a series of static load-case calculations with FETire/static. These calculations are controlled by a simulation script, and run fully automatic. They compute the static tire forces and moments under several different conditions, like

- vertical deflection on a flat surface,
- vertical deflection on a transversally and a longitudinally oriented cleat,
- vertical deflection with different camber angles on flat surface and on cleats,
- lateral wheel displacement, at a high friction value,
- longitudinal wheel displacement, at a high friction value, and
- wheel rotation about vertical axis, at a high friction value.

All these computations are performed with several different deflection values and inflation pressures. The resulting static data is completed by the first resonance frequencies and modal damping values, computed with FETire/modal. Here, the same tire design data is used as with FETire/static. Some of the results are used to generate an FTire input file, some others to validate the respective FTire model. A full cycle of an FTire parameterization with FTire/calc only takes about 1 to 10 min CPU time, depending on the chosen grid-size of the FETire mesh, and thus the accuracy that is achieved.

FTire/fit, the second tool, assists with a procedure of type (3). It provides several optimization routines that minimize the least squares distance between cleat test measurements and respective simulations with FTire. In addition, FTire/fit assists in repeatedly and rapidly performing other script-based validation simulations, like side-force or μ-slip characteristics. Typically, the optimization step will require some 1000 evaluations of the objective function (which is the least squares sum). Each evaluation, in turn, will perform a certain number (10, say) of cleat test simulations at different rolling speeds, cleat geometries, cleat orientations, wheel loads, camber angles, and inflation pressures.

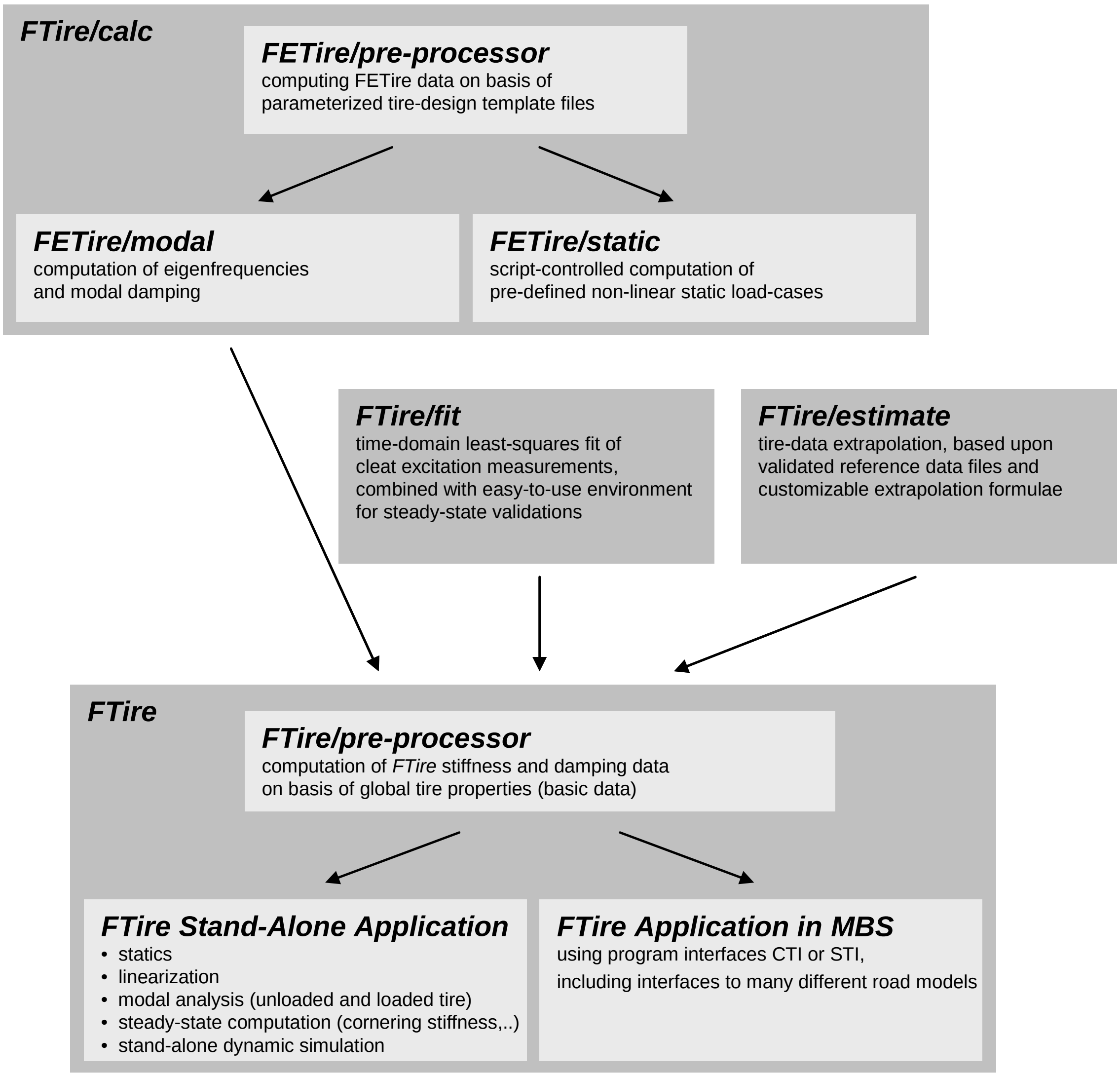

Fig. 22: FTire Parameterization and Application Tools

A typical cleat test will provide relevant tire response signals for a time span of 200 ms, and the FTire real-time factor (RTF) is close to 3 (cf. figure 14). Thus, the required CPU time of such a parameter identification cycle is of the order of magnitude of at least

$$t_{CPU} = n_{eval} \cdot n_{cleat\ tests} \cdot t_{sim} \cdot \mathrm{RTF} \geq 1000 \cdot 10 \cdot 0.2 \cdot 3\ \mathrm{s} = 100\,\mathrm{min}\,.$$

This number is only a lower bound, because in addition an FTire pre-processing step has to be performed for each objective evaluation.

FTire/fit is not meant to be a ‘black-box tool’, which provides results by few mouse-clicks only. Rather, it requires a certain expertise to select and prepare appropriate cleat test measurements, and to decide what parameters should be determined by what kind of cleat tests, and in what sequence. Moreover, it requires expertise as well to assess whether or not the optimization really is successful, or should be aborted due to non-convergence, or convergence against a non-global minimum. As with all applications of computer optimization, there is no guarantee at all that the global optimum really was found. This introduces uncertainty about the quality of the result, which only can be overcome by having experience with previous similar computations. It seems to be logical to only use a standardized measuring procedure, and to use FTire/fit always in the same way in conjunction with this procedure. This is the best way to achieve comparable FTire data for different tires.

Finally, there is a third tool (FTire/estimate, figure 23) available which implements a procedure of type (5). FTire/estimate uses a well-validated FTire data file, representing a whole family of similar tires. Using this tire, it relates its stiffness and modal data to the respective values of other tires in the family, which might differ in

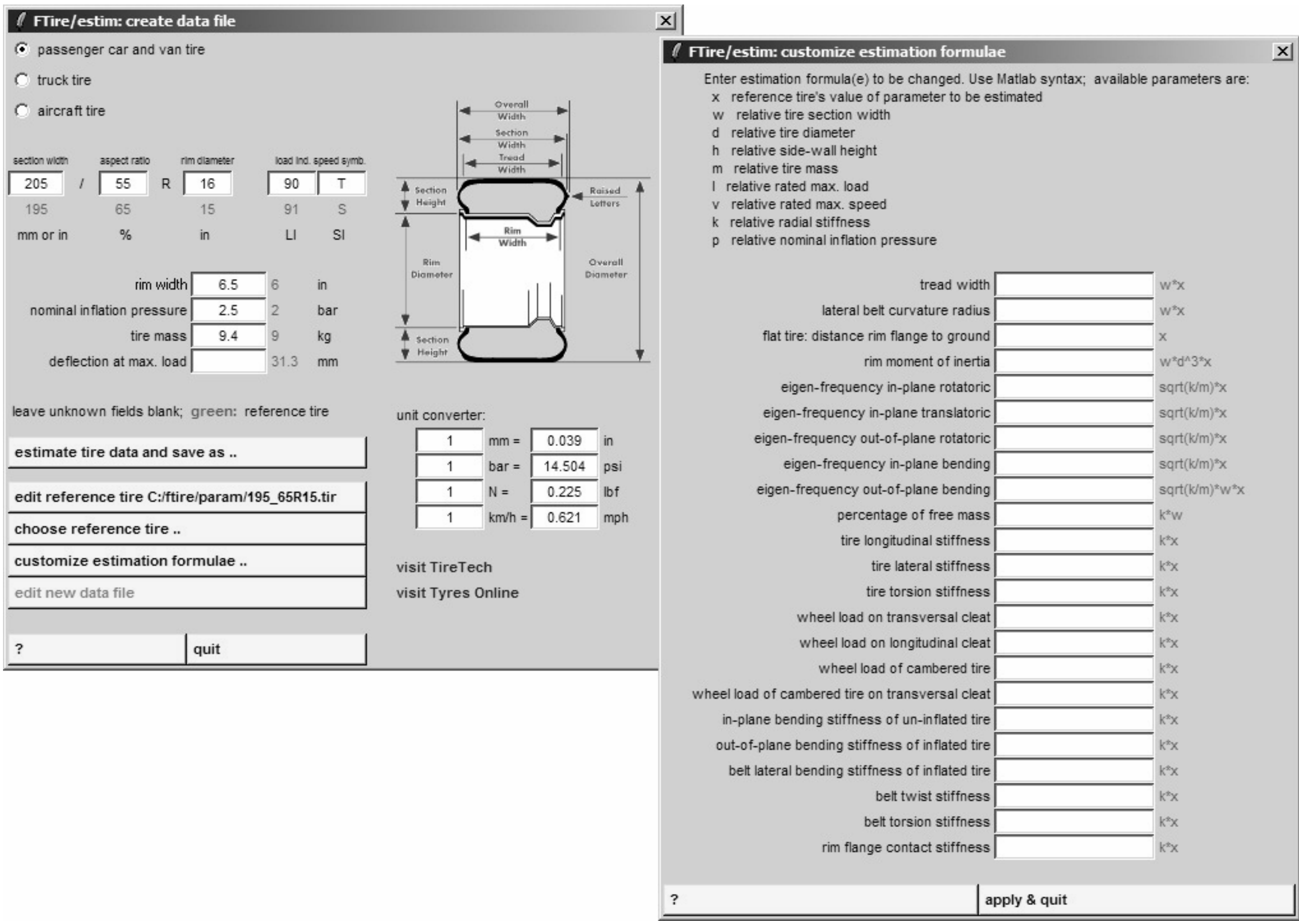

Fig. 23: FTire/estimate User Interface (GUI) Showing Default Estimation Formulae

section width, aspect ratio, rim size, mass, maximum load, maximum speed, radial stiffness, or nominal inflation pressure.

This relation is described in terms of functional dependencies: the changes in static and modal tire data are functions of the change in one or more influence parameters. These influence parameters are: tire section width, tire diameter, side-wall height, tire mass, rated maximum load, rated maximum speed, radial stiffness, and nominal inflation pressure.

Clearly, these data items are not all independent on each other. Some of them are provided by the estimation program for completeness only. For example, it might be more natural to express the dependency of an eigenvalue on mass than on tire size, even if both will change simultaneously. In any case, it is sufficient to use only the most relevant influence parameters in the formulae.

The influence functions used by default are based upon simple mechanical analogy considerations. However, they can be easily customized. A user might wish to enhance his copy of FTire/estimate, based upon his experience, in the sense of an expert system. Clearly, this experience can be easily completed by studies with detailed FE models, or by evaluating respective measurements.

References

[1] Gipser M.: *DNS-Tire, ein dynamisches, räumliches nichtlineares Reifenmodell*. In: Reifen, Fahrwerk, Fahrbahn. VDI Berichte 650, pp.115-135. VDI Verlag Düsseldorf 1987

[2] Gipser M.: *DNS-Tire, a Dynamic Nonlinear Spatial Tire Model In Vehicle Dynamics*. Proc. 2nd Workshop on Road-Vehicle-Systems and Related Mathematics, ISI, Torino Italy, 1987, ed. Neunzert, H. Teubner Stuttgart 1989

[3] Ammon D.; Gipser M.; Rauh J.; Wimmer J.: *Effiziente Simulation der Gesamtsystemdynamik Reifen-Achse-Fahrwerk*. In: Reifen, Fahrwerk, Fahrbahn. VDI-Berichte 1224. VDI Verlag Düsseldorf 1995

[4] Gipser M.: *DNS-Tire 3.0 - die Weiterentwicklung eines bewährten strukturmechanischen Reifenmodells*. In: Darmstädter Reifenkolloquium, VDI Berichte 512, pp.52-62. VDI Verlag Düsseldorf 1996

[5] Gipser M., Hofer R., Lugner P.: *Dynamical Tire Forces Response to Road Unevenness*. Proc. 2nd Int. Coll. On Tyre Models for Vehicle Dynamic Analysis. Supplement to Vehicle System Dynamics, Vol.27. Swets & Zeitlinger Lisse 1997

[6] Gipser M.: *Reifenmodelle für Komfort- und Schlechtwegsimulationen*. Proc. 7. Aachener Kolloquium Fahrzeug- und Motorentechnik. IKA, RWTH Aachen, VDI Verlag 1998

[7] Van Oosten J.J.M; Unrau H.J.; Riedel G.; Bakker E.: *TYDEX Workshop: Standardisation of Data Exchange in Tyre Testing and Tyre Modelling*. In: Tyre Models for Vehicle Dynamic Analysis. Supplement to Vehicle System Dynamics, Vol.27. Swets&Zeitlinger Lisse 1997

[8] Gipser M.: *FTire, a New Fast Tire Model for Ride Comfort Simulations*. International ADAMS User's Conference Berlin 1999

[9] Gipser M.: *ADAMS/FTire - A Tire Model for Ride & Durability Simulations*. ADAMS User's Conference Tokyo 2000

[10] Riepl A.; Reinalter W.; Fruhmann G.: *Rough Road Simulation with Tire Model RMOD-K and FTire*. Proc. 18th IAVSD Symposium. Kanagawa Institute of Technology, Atsugi-shi Japan 2003

[11] Gipser M.: *FTire Documentation.* Available from http://www.ftire.com